DFPD-00/TH/17

Signatures of massive sgoldstinos at hadron colliders

Elena Perazzi[1]
Dipartimento di Fisica, Università di Padova, I-35131 Padua, Italy
Giovanni Ridolfi[2]
INFN, Sezione di Genova, I-16146 Genoa, Italy
and
Fabio Zwirner[3]
INFN, Sezione di Padova, I-35131 Padua, Italy

Abstract

In supersymmetric extensions of the Standard Model with a very light gravitino, the effective theory at the weak scale should contain not only the goldstino $\tilde{G}$, but also its supersymmetric partners, the sgoldstinos. In the simplest case, the goldstino is a gauge-singlet and its superpartners are two neutral spin–0 particles, S and P. We study possible signals of massive sgoldstinos at hadron colliders, focusing on those that are most relevant for the Tevatron. We show that inclusive production of sgoldstinos, followed by their decay into two photons, can lead to observable signals or to stringent combined bounds on the gravitino and sgoldstino masses. Sgoldstino decays into two gluon jets may provide a useful complementary signature.

[1]e-mail address: perazzi@pd.infn.it
[2]e-mail address: ridolfi@ge.infn.it
[3]e-mail address: zwirner@pd.infn.it

1. Introduction

Sgoldstinos are the supersymmetric partners of the goldstino $\tilde{G}$, and, in supersymmetric models with a very light gravitino [1]–[4], are expected to be part of the effective theory at the weak scale. In the simplest case, the R–odd goldstino is a gauge singlet, and its R–even superpartners are two neutral spin–0 particles, S (CP–even) and P (CP–odd): in the following, we will use the generic symbol ϕ to denote any of the two sgoldstino states. If the sgoldstino masses m_ϕ and the supersymmetry-breaking scale $\sqrt{F}$ are not too large, [1] sgoldstino production and decay may be detectable at the present collider energies.

Previous studies of sgoldstino phenomenology at colliders [5] were performed under the very restrictive assumption of negligible sgoldstino masses. In a recent paper [6], we started a systematic investigation of the possible phenomenological signatures of massive sgoldstinos, concentrating on e^+e^- colliders and in particular on LEP. We showed that the study of processes such as $e^+e^- \to \gamma\phi$, $Z\phi$ or $e^+e^-\phi$, followed by ϕ decaying into two gluon jets, can explore virgin land in the parameter space of models with a superlight gravitino. This was confirmed by a subsequent experimental analysis [7], where (using not only the two-gluon decay mode, but also the two-photon one, as suggested by previous LEP searches [8]) new stringent combined bounds on the gravitino and sgoldstino masses were derived.

In the present work, we extend the study of the phenomenology of massive sgoldstinos to the case of hadron colliders, with emphasis on the Tevatron ($p\overline{p}$; $\sqrt{S} = 1.8$ TeV and $L \sim 100$ pb^{-1} in run I; $\sqrt{S} = 2$ TeV and $L \sim 2$ fb^{-1} in run II). Our study is organized as follows. In sect. 2, we complete the discussion of the sgoldstino effective couplings and branching ratios given in [6], to encompass a range of sgoldstino masses extending above the $t\bar{t}$ threshold. In sect. 3, we discuss the mechanisms for sgoldstino production at hadron colliders, giving explicit formulae for the relevant partonic cross-sections and showing some representative numerical results. In sect. 4, we review the resulting signals at the Tevatron and we attempt a first discussion of the discovery potential of the different channels, leaving a more detailed analysis to our experimental colleagues. We show that inclusive production of sgoldstinos, followed by their decay into two photons, can lead to observable signals or to stringent combined bounds on the gravitino and sgoldstino masses. The sgoldstino decay mode into two gluon jets, dominant over most of the parameter space but plagued by large backgrounds, may provide a useful complementary signature when gluinos are much heavier than the electroweak gauginos and higgsinos. Associated production with an electroweak gauge boson (γ, W, Z) and/or other decay modes ($\gamma Z, ZZ, WW, \tilde{G}\tilde{G}, t\bar{t}$) do not lead in general to an increased sensitivity.

To conclude this introduction, we would like to alert the reader on some simplifying assumptions underlying our analysis, and on the analogies between sgoldstinos and other

[1] We remind the reader that the supersymmetry–breaking scale $\sqrt{F}$ can be put in one–to–one correspondence with the gravitino mass $m_{3/2}$, via the relation $F = \sqrt{3}\, m_{3/2} M_P$, where $M_P \equiv (8\pi G_N)^{-1/2} \simeq 2.4 \times 10^{18}$ GeV is the Planck mass.

hypothetical spin–0 particles, such as the neutral Higgs bosons of the Standard Model (SM) or its Minimal Supersymmetric extension (MSSM). As in [6], we will perform our study assuming that there is no mixing between sgoldstinos and Higgs bosons, and that R–odd MSSM particles and Higgs bosons [2] are sufficiently heavy not to play a rôle in sgoldstino production and decay. This should be taken as a benchmark case, which may be further generalized by including an exhaustive treatment of the interplay between $SU(2) \times U(1)$ and supersymmetry breaking [10]. Whenever possible, however, we will compare the properties of our 'pure' sgoldstinos with the properties of the 'pure' SM or MSSM Higgs bosons: in the case of non–negligible mixing, we may expect intermediate properties. In this respect, sgoldstinos represent a motivated and well-defined addition to a long list of other hypothetical spin–0 particles ('bosonic Higgs', 'coloron', ...) that have been proposed with various theoretical motivations, and are often used in data analyses to parametrize some of the searches for new physics. Since the indirect evidence for the SM (or the MSSM) as the correct and complete theory at the weak scale is far from conclusive [11], we believe that more exotic possibilities such as sgoldstinos still deserve to be taken seriously, even on purely phenomenological grounds. On the theoretical side, it is interesting to notice that sgoldstinos bear some similarities with the spin–0 fields arising from the metric (and antisymmetric tensors) of extra space-time dimensions in some 'brane-world' scenarios [12, 13], whose collider phenomenology has been recently discussed [14]. These similarities could be investigated more closely, leading perhaps to a more unified picture, if progress were made in the discussion of the breaking of supersymmetry and of the electroweak symmetry in this context.

2. Sgoldstino effective couplings and branching ratios

The general theoretical framework for the discussion of sgoldstino phenomenology was reviewed in [6], to which we refer the reader. Sgoldstino effective interactions and branching ratios were also discussed in [6], with emphasis on the sgoldstino mass range kinematically accessible at LEP, $m_\phi \lesssim 200$ GeV. It was shown that the sgoldstino couplings to gauge boson pairs can be parametrized by the supersymmetry-breaking scale $\sqrt{F}$, by the gaugino masses (M_3, M_2, M_1) and by a mass parameter μ_a, associated with the charged higgsino and the antisymmetric combination of neutral higgsinos. To extend the discussion to higher sgoldstino masses, which may be phenomenologically relevant at the Tevatron (or eventually at the LHC), we need only a more detailed discussion of the $t\bar{t}\phi$ effective couplings and of $\phi \to t\bar{t}$ decays.

As discussed in [4], the Yukawa couplings of sgoldstinos to leptons and light quarks (for our purposes, all but the top quark) are expected to be suppressed by a factor $m_f/\sqrt{F}$,

[2] We remind the reader that, in models with a very light gravitino, the MSSM upper bound [9] on the mass of the lightest Higgs boson can be grossly violated [3].

where m_f is the fermion mass. We then expect these couplings to be important only for the top quark, and parametrize them as follows:

$$\mathcal{L}_{\phi t\bar{t}} = -\frac{m_t A_S}{\sqrt{2}F}\left(S t t^c + \text{h.c.}\right) - \frac{m_t A_P}{\sqrt{2}F}\left(iP t t^c + \text{h.c.}\right) , \tag{1}$$

where we used two-component spinors in the notation of [6], and A_S, A_P are free parameters with the dimension of a mass. Since $A_S + A_P = 2A_t$, where $\delta m^2 = m_t A_t$ is the off-diagonal element in the mass matrix for the stop squarks, we expect A_S and A_P to be of the order of the other supersymmetry-breaking masses in the strongly interacting sector of the theory. Notice that the $St\bar{t}$ coupling is identical in form to the coupling of the SM Higgs, and can be obtained from the latter by performing the substitution

$$\frac{g}{2m_W} \longrightarrow \frac{A_S}{\sqrt{2}F} . \tag{2}$$

Similarly, the $Pt\bar{t}$ coupling can be obtained from the coupling of the SM Higgs by inserting, in four-component notation, a γ_5 matrix in the fermion bilinear, and by performing the substitution

$$\frac{g}{2m_W} \longrightarrow \frac{iA_P}{\sqrt{2}F} . \tag{3}$$

Alternatively, the $Pt\bar{t}$ coupling can be also obtained from the $At\bar{t}$ coupling of the MSSM by performing the substitution of eq. (3) and by making the choice $\tan\beta = 1$. Notice also that, in general, we can have $A_S \neq A_P$. In the following, however, we will make the simplifying assumption $A_S = A_P \equiv A_t$, and, whenever needed for numerical examples, the representative choice $A_t = M_3$. From eq. (1) we find

$$\Gamma(S \to t\bar{t}) = \frac{3m_t^2 A_S^2 m_S}{16\pi F^2}\left(1 - \frac{4m_t^2}{m_S^2}\right)^{3/2} , \quad \Gamma(P \to t\bar{t}) = \frac{3m_t^2 A_P^2 m_P}{16\pi F^2}\left(1 - \frac{4m_t^2}{m_P^2}\right)^{1/2} . \tag{4}$$

Notice the different exponent for the CP-even and the CP-odd state, as in the MSSM.

We are now ready to extend the discussion of the sgoldstino branching ratios to the mass range of interest at the Tevatron. We will focus our attention on the dependences on m_ϕ and $\sqrt{F}$, by making for the remaining parameters the two representative choices given in Table 1. The corresponding chargino and neutralino masses (in GeV) are approx-

	M_3	M_2	M_1	μ_a	A_S	A_P
(a)	400	300	200	300	400	400
(b)	350	350	350	350	350	350

Table 1: Two representative choices for the mass parameters affecting the sgoldstino effective couplings. All masses are expressed in GeV.

imately $(220, 380)$ and $(175, 240, 385)$ for case (a), $(270, 430)$ and $(260, 350, 440)$ for case

(b). There is of course a fourth neutralino, the symmetric higgsino combination, whose mass is controlled by an independent parameter μ_s, and does not affect the sgoldstino couplings. For most values of $\sqrt{F}$ to be considered in the following, the two parameter choices of Table 1 should be comfortably compatible with the present experimental limits on R-odd supersymmetric particles, coming from LEP and Tevatron searches. For sufficiently large values of the sgoldstino masses, we should also consider sgoldstino decays into pairs of neutralinos, charginos or gluinos. However, the relevant couplings are controlled not only by the parameters of Table 1, but also by μ_s, by the Higgs boson masses and by other parameters not related with the spectrum [10]. In the following, we will always assume that the corresponding branching ratios can be safely neglected. In the region of sgoldstino masses considered in this paper, the only kinematically allowed decays could be those into the lightest neutralinos and charginos. For a wide range of the remaining parameters, these decays are sufficiently suppressed by the phase space and other factors, so that our discussion of the dominant decay modes remains a good approximation.

Since all the partial widths for two–body decays are proportional to F^{-2}, the dependence on F drops out of the discussion of the ϕ branching ratios. The latter are shown in Figs. 1 and 2, as functions of m_ϕ, for the two cases of S and P and for the two parameter choices of Table 1. We can see that the differences in the couplings of S and P to the massive weak bosons and to the top quark do not have an important impact on the branching ratios. For both S and P, the most important decay mode is the one into gluons, with the one into goldstinos becoming competitive only for very large sgoldstino masses. In the whole mass range up to 1 TeV, decays into electroweak bosons are suppressed, at the level of 10% or less: as we will see, however, these modes could still be relevant for hadron collider searches, because of the much smaller backgrounds of the resulting signals.

As already discussed in [6], another important quantity is the total ϕ width, Γ_ϕ, controlled by the ratios between the relevant mass parameters and the supersymmetry-breaking scale. Large values of these ratios correspond to broad, strongly coupled sgoldstinos: to keep the particle interpretation and the validity of our approximations, we must require, among the other things, $\Gamma_\phi/m_\phi \ll 1$. To compare signal and background in the narrow-width approximation, we must impose more stringent constraints: $\Gamma_\phi/m_\phi < 10^{-1}$ when discussing decays into jets, $\Gamma_\phi/m_\phi <$ few $\times\, 10^{-2}$ when discussing decays into photons. We then show in Fig. 3 contours corresponding to constant values of Γ_ϕ/m_ϕ in the $(m_\phi, \sqrt{F})$-plane, for the two parameter choices of Table 1. Since the curves for $\phi = S$ and $\phi = P$ are almost indistinguishable, we draw both of them simultaneously. As we will see in sects. 3 and 4, while the region of parameter space of experimental interest at LEP is such that sgoldstinos can always be treated as very narrow resonances, this is not necessarily the case at the Tevatron.

As a final remark on the branching ratios, we remind the reader that our computations have been performed at leading order. In analogy with the case of the SM and MSSM neutral Higgs bosons, we expect the NLO QCD corrections to increase the partial width into gluons by a factor $K \sim 1.6$. Since the two-gluon decay mode is the dominant one,

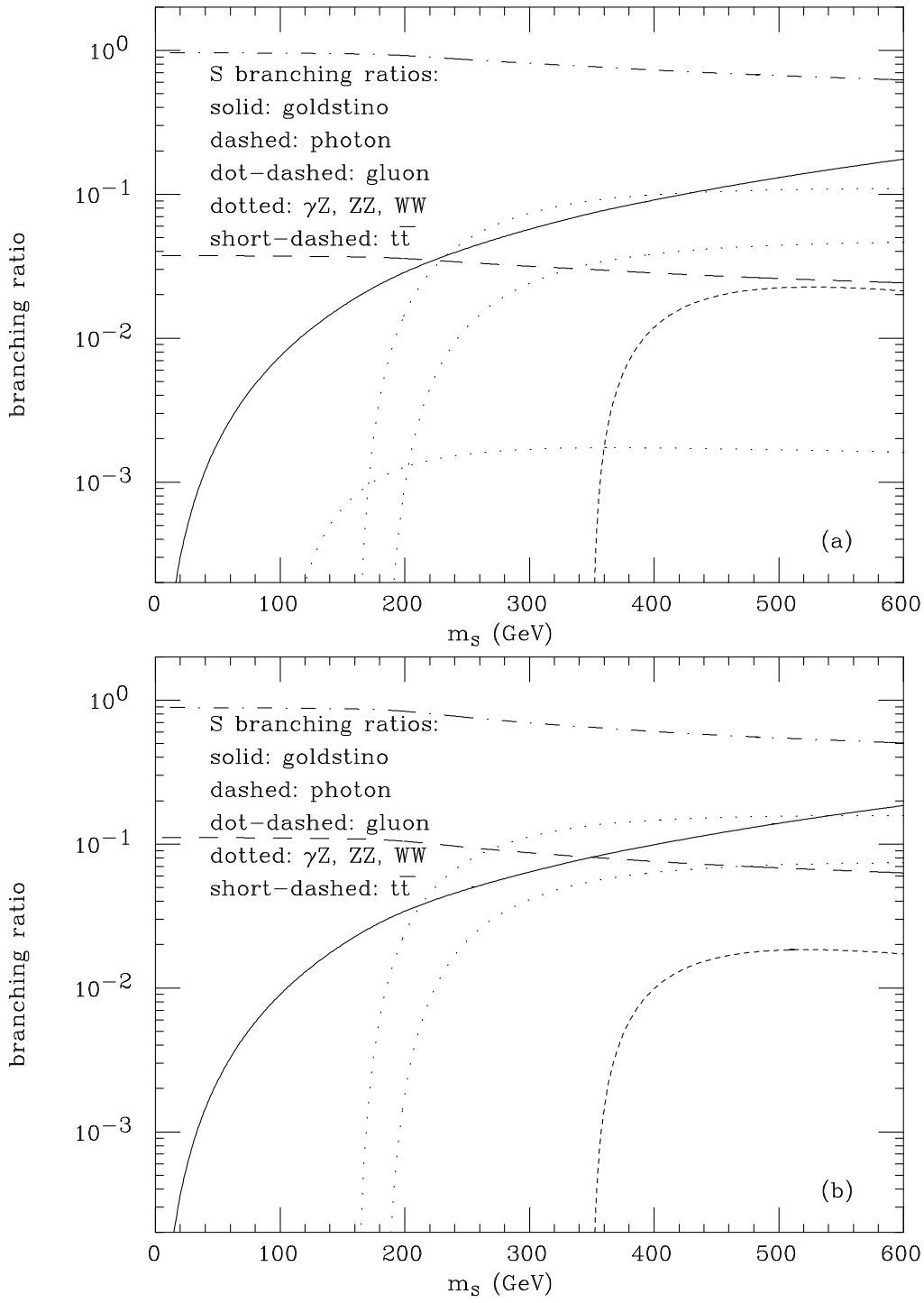

Figure 1: *The S branching ratios, as functions of m_S, for the two parameter choices of Table 1.*

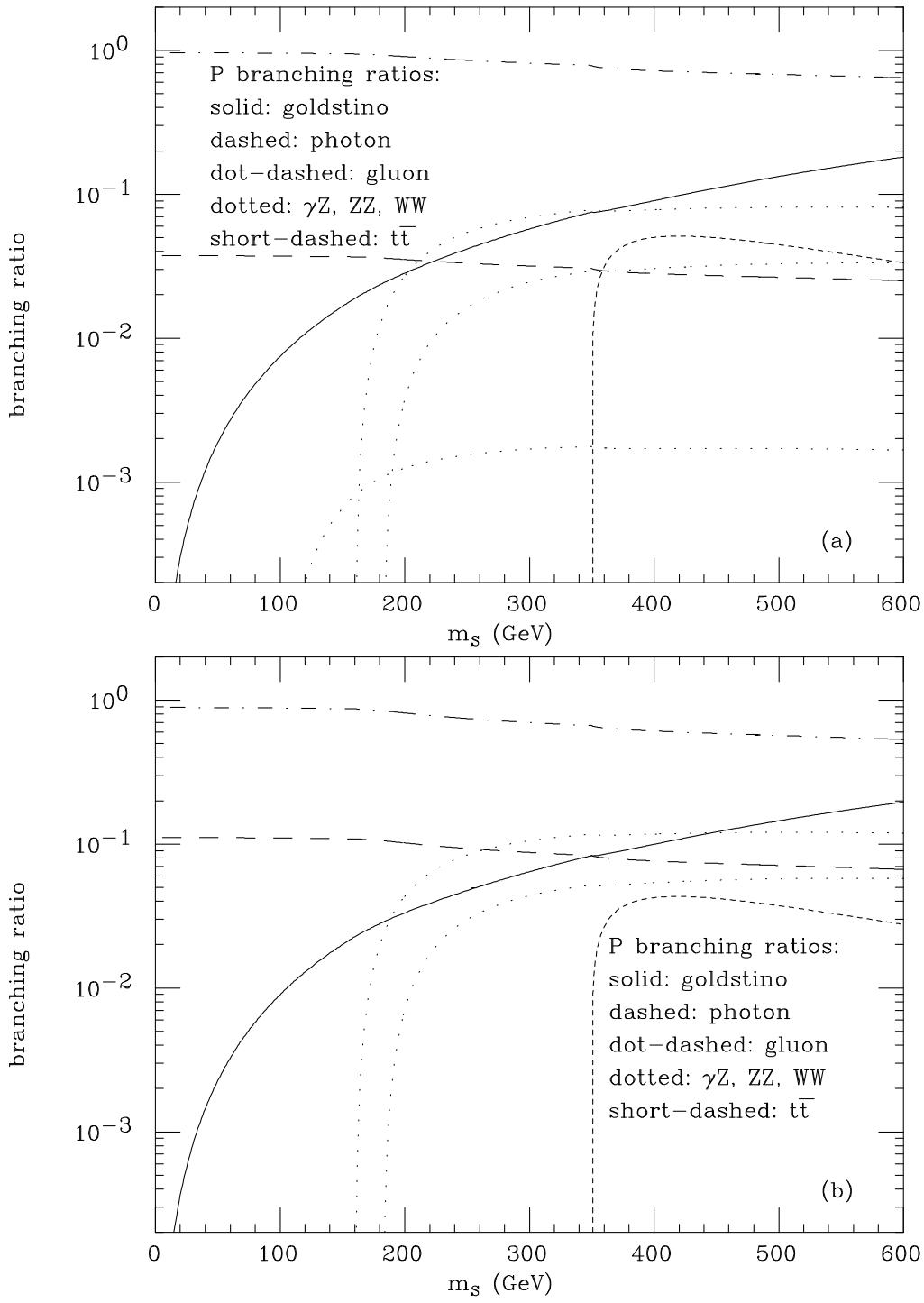

Figure 2: *The P branching ratios, as functions of m_P, for the two parameter choices of Table 1.*

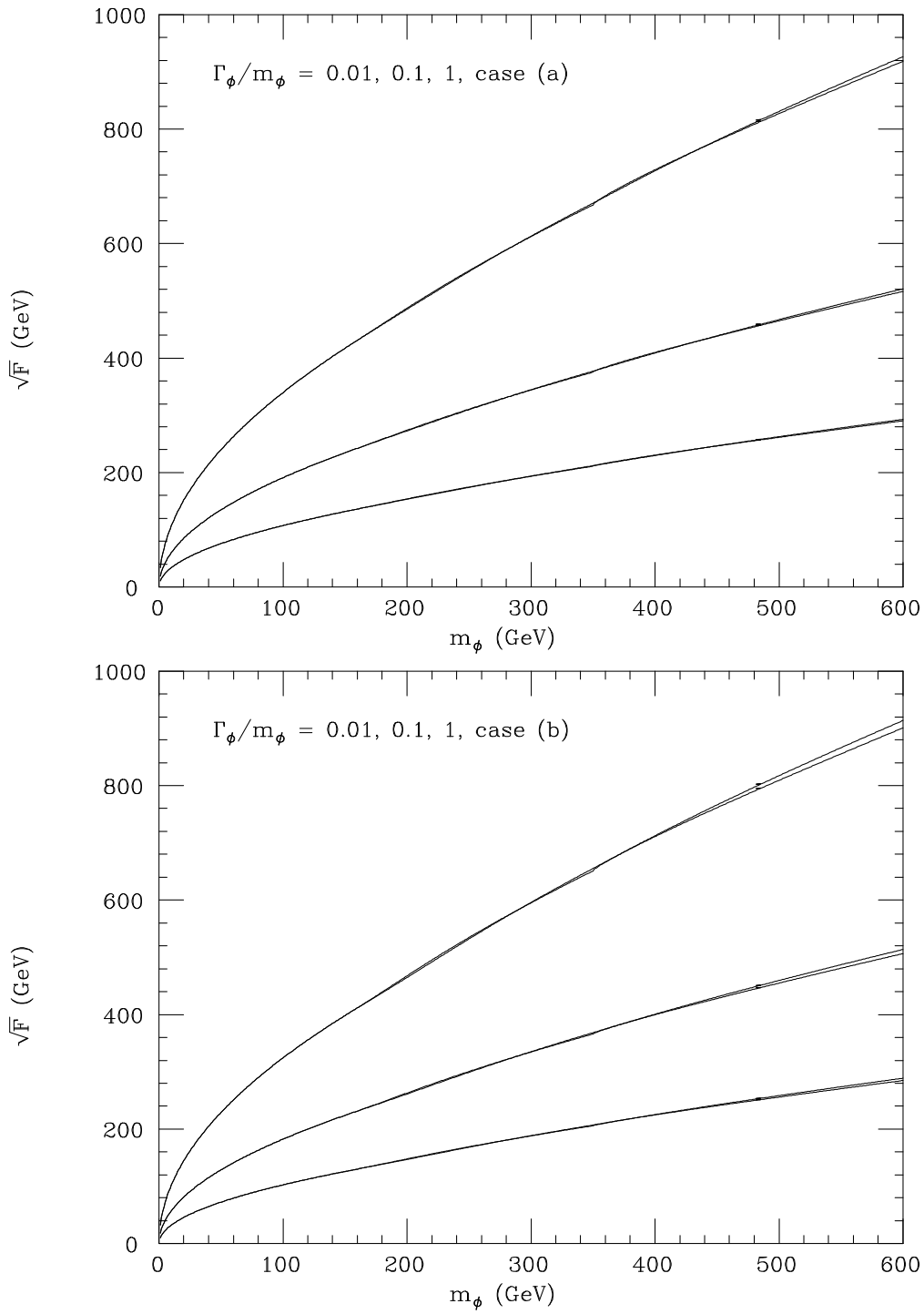

Figure 3: *Lines corresponding to fixed values of* Γ_ϕ/m_ϕ *in the* $(m_\phi, \sqrt{F})$ *plane, for the two parameter choices of Table 1. Both* $\phi = S$ *and* $\phi = P$ *are considered.*

this may lead to a non-negligible suppression of the rarer decay modes. When important, this will be taken into account in the phenomenological discussion of sect. 4.

3. Production cross-sections

The possible parton-level mechanisms for sgoldstino production at hadron colliders are very similar to those for the SM Higgs and can be easily classified:

$$g + g \longrightarrow \phi\,, \tag{5}$$

$$q + \overline{q} \longrightarrow V + \phi\,, \tag{6}$$

$$q + \overline{q} \longrightarrow q + \overline{q} + \phi\,, \tag{7}$$

$$g + g \text{ or } q + \overline{q} \longrightarrow t + \overline{t} + \phi\,, \tag{8}$$

where q denotes any quark flavour and V any of the electroweak vector bosons, including the photon. We briefly discuss here the corresponding cross-sections, giving some numerical examples for the Tevatron. In the case of the SM Higgs, the dominant Higgs production mechanism at the Tevatron is the one of eq. (5), with those of eqs. (6) and (7) suppressed by roughly one order of magnitude, and the one of eq. (8) suppressed by roughly an additional order of magnitude in the mass region of interest. An important rôle in these hierarchies is played by the fact that the SM Higgs couplings to WW and ZZ arise at the tree-level and are unsuppressed, whereas the couplings to gg (and $\gamma\gamma$) arise at the one-loop level, and are therefore considerably suppressed. This compensates in part the hierarchy between strong and electroweak interactions, and allows for the subdominant production mechanisms to be of phenomenological interest. In contrast with the SM Higgs, all sgoldstino couplings to vector boson pairs are essentially on the same footing. The result, which could already be guessed from our study of the branching ratios, is the following: the practical relevance of the subdominant production mechanisms at hadron colliders will be much smaller in the case of sgoldstinos than in the case of the SM and MSSM neutral Higgs bosons.

To produce numerical examples, we will always adopt the CTEQ5 parametrization of the parton distribution functions [15] with $\Lambda_5 = 226$ MeV, corresponding to $\alpha_S(m_Z) = 0.118$. Our results are summarized in Fig. 4, which displays some of the lowest-order sgoldstino production cross-sections, as functions of the sgoldstino mass, for $p\overline{p}$ collisions at $\sqrt{S} = 2$ TeV. The cross-sections of Fig. 4 have been obtained for $\sqrt{F} = 1$ TeV. Since they are all proportional to $1/F^2$, the cross-sections for any other value of $\sqrt{F}$ can be obtained by a simple rescaling of the values of Fig. 4. Cases (a) and (b) correspond as usual to the two representative parameter choices of Table 1. For simplicity, only the case of $\phi = S$ has been considered. On the scale of Fig. 4, the results for the case $\phi = P$ are very similar.

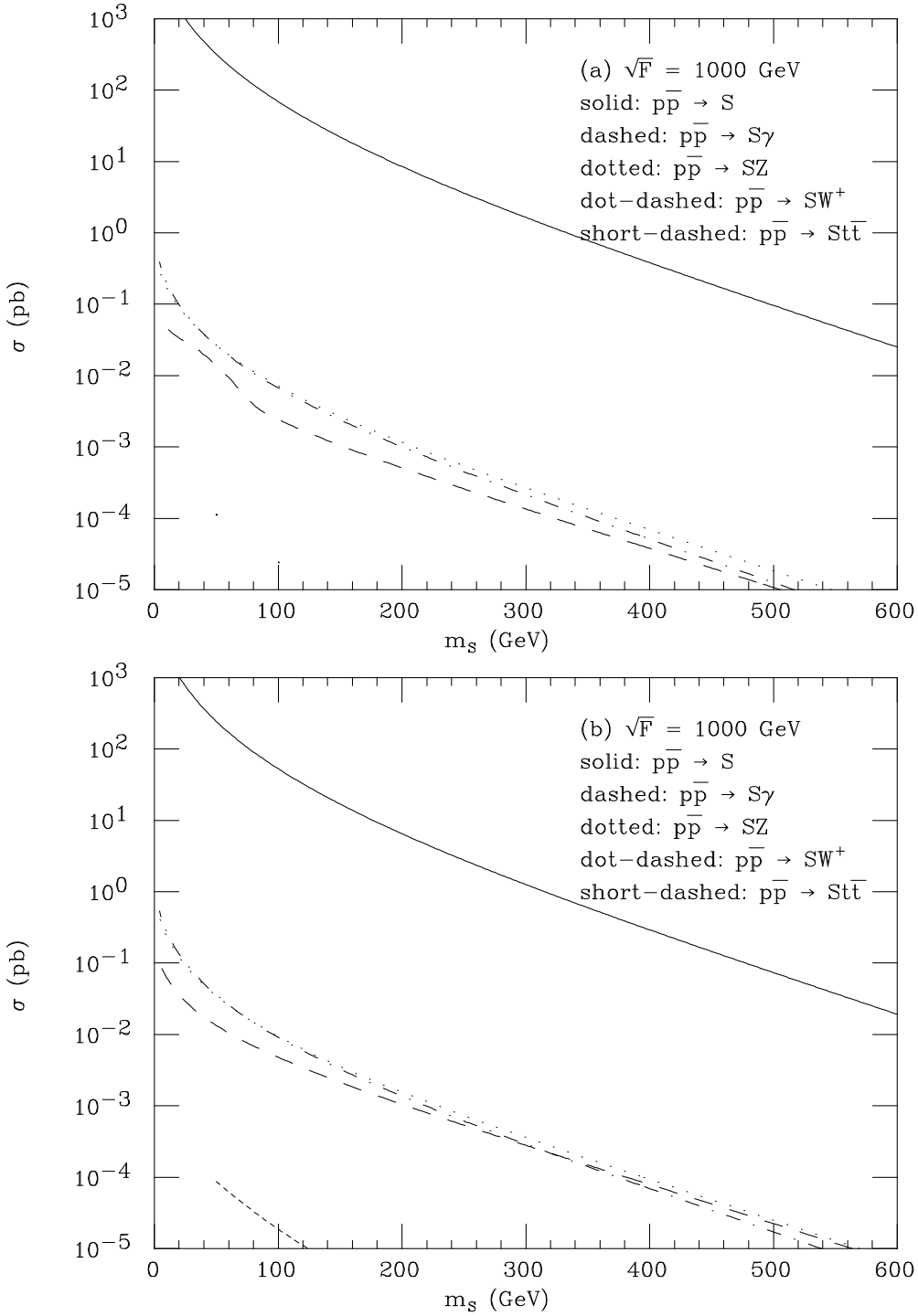

Figure 4: *Lowest-order sgoldstino production cross-sections at the Tevatron ($p\overline{p}$, $\sqrt{S}$ = 2 TeV) as functions of the sgoldstino mass and for $\phi = S$. Cases (a) and (b) correspond to the two parameter choices of Table 1.*

Gluon-gluon fusion

Since the sgoldstino couplings to light quarks are suppressed by the corresponding quark masses (as it is the case for the SM Higgs), whilst the effective gluon-gluon-sgoldstino couplings are proportional to M_3/F, the dominant production mechanism of massive sgoldstinos at hadron colliders is in general gluon-gluon fusion, eq. (5). To lowest order, the partonic cross-section can be expressed in terms of the gluonic width of the sgoldstino,

$$\sigma(g\,g \to \phi) = \sigma_0\; m_\phi^2\; \delta(s - m_\phi^2)\,, \qquad \sigma_0 = \frac{8\pi^2}{m_\phi^3}\,\Gamma(\phi \to g\,g)\,, \tag{9}$$

where $\sqrt{s}$ is the total energy in the centre-of-mass frame of the incoming partons. With the lowest-order expression for $\Gamma(\phi \to g\,g)$ given in [6], we find

$$\sigma_0 = \frac{\pi M_3^2}{32 F^2}\,. \tag{10}$$

The lowest-order proton-antiproton cross-section is then, in the narrow-width approximation,

$$\sigma(p\overline{p} \to \phi) = \sigma_0\; \tau \int_\tau^1 \frac{dx}{x} f_g(x, m_\phi^2) f_g(\tau/x, m_\phi^2)\,, \tag{11}$$

where $\tau = m_\phi^2/S$, $\sqrt{S}$ is the total centre-of-mass energy of the proton-antiproton system, and $f_g(x, Q^2)$ is the gluon distribution function, the same for proton and antiproton. An identical formula holds for the proton-proton cross-section. Notice that the above formulae are very similar in form to those for the production of a light SM Higgs boson. The only difference is that for the Higgs

$$\sigma_0 = \frac{G_F \alpha_s^2}{288\sqrt{2}\pi}\,. \tag{12}$$

For a heavy Higgs, one must correct for the form factor originating from the top-quark loop and for the finite Higgs width, whilst the present approximation should be also applicable to heavy sgoldstinos, provided that $m_\phi M_3/F \lesssim 1$. The formal analogy with Higgs production also allows to include the NLO QCD corrections, by adapting the computation of [16]. For our present purposes, it is sufficient to work at the leading non-trivial order. In the phenomenological discussion of sect. 4, however, we will include the most important QCD corrections by making the rough approximation $\sigma_{NLO} = K\,\sigma$, with $K \simeq 2$.

Associated $\phi\gamma$ production

In analogy with the process $e^+e^- \to \phi\gamma$, already considered in [6], we can consider the process $q\overline{q} \to \phi\gamma$. This process is made possible by the existence of effective $\gamma\gamma\phi$ and $\gamma Z\phi$ couplings, whose explicit form can be found in [6]. They are controlled by the ratios $M_{\gamma\gamma}/F$ and $M_{\gamma Z}/F$, respectively, where $M_{\gamma\gamma} = M_1 \cos^2\theta_W + M_2 \sin^2\theta_W$ and $M_{\gamma Z} = (M_2 - M_1)\sin\theta_W \cos\theta_W$. At the partonic level and before including QCD corrections, there are only two Feynman diagrams to compute, corresponding to s-channel γ and Z

exchange. Neglecting both the quark masses and the Z width, the differential cross-section for a given quark flavour q is

$$\frac{d\sigma}{d\cos\theta}(q\overline{q}\to\phi\gamma) = \frac{|\Sigma_{\phi\gamma}|^2 s}{64\pi N_c F^2}\left(1-\frac{m_\phi^2}{s}\right)^3\left(1+\cos^2\theta\right), \tag{13}$$

where $N_c = 3$ is a color factor,

$$|\Sigma_{\phi\gamma}|^2 = \frac{e^2Q_q^2M_{\gamma\gamma}^2}{2s} + \frac{g_Z^2(v_q^2+a_q^2)M_{\gamma Z}^2 s}{2(s-m_Z^2)^2} + \frac{eQ_qg_Zv_qM_{\gamma\gamma}M_{\gamma Z}}{(s-m_Z^2)}, \tag{14}$$

$v_q = T_{3q}/2 - Q_q\sin^2\theta_W$, $a_q = -T_{3q}/2$, $T_{3u} = T_{3c} = T_{3t} = -T_{3d} = -T_{3s} = -T_{3b} = 1/2$, $Q_u = Q_c = Q_t = +2/3$, $Q_d = Q_s = Q_b = -1/3$, $g_Z = e/(\sin\theta_W\cos\theta_W)$, and θ is the scattering angle in the centre-of-mass frame of the colliding partons.

Associated ϕZ production

Another process to be considered is $q\overline{q}\to\phi Z$, analogous to the process $e^+e^-\to\phi Z$ considered in [6]. For $\phi = P$, the differential cross-section is

$$\frac{d\sigma}{d\cos\theta}(q\overline{q}\to PZ) = \frac{|\Sigma_{PZ}|^2}{32\pi N_c s^2F^2}\sqrt{(s-m_P^2-m_Z^2)^2-4m_P^2m_Z^2}, \tag{15}$$

where

$$|\Sigma_{PZ}|^2 = \left(\frac{e^2Q_q^2M_{\gamma Z}^2}{2s} + \frac{g_Z^2(v_q^2+a_q^2)M_{ZZ}^2 s}{2(s-m_Z^2)^2} + \frac{eQ_qg_Zv_qM_{\gamma Z}M_{ZZ}}{(s-m_Z^2)}\right)\left(t^2+u^2-2m_P^2m_Z^2\right), \tag{16}$$

and (t,u) are the usual Mandelstam variables for two-body scattering. The cross-section for $\phi = S$ has some additional complications, because, as discussed in [6], the SZZ coupling has an additional dependence on the higgsino mass parameter μ_a:

$$\frac{d\sigma}{d\cos\theta}(q\overline{q}\to SZ) = \frac{|\Sigma_{SZ}|^2}{32\pi N_c s^2F^2}\sqrt{(s-m_S^2-m_Z^2)^2-4m_S^2m_Z^2}, \tag{17}$$

where

$$\begin{aligned}
|\Sigma_{SZ}|^2 &= \left[\frac{e^2Q_q^2M_{\gamma Z}^2}{2s} + \frac{g_Z^2(v_q^2+a_q^2)M_{ZZ}^2 s}{2(s-m_Z^2)^2} + \frac{eQ_qg_Zv_qM_{\gamma Z}M_{ZZ}}{s-m_Z^2}\right]\left[t^2+u^2+2m_Z^2(2s-m_S^2)\right] \\
&+ \frac{g_Z^2\mu_a^2m_Z^4(v_q^2+a_q^2)}{(s-m_Z^2)^2}\left(2s-m_S^2+\frac{tu}{m_Z^2}\right) \\
&+ \frac{g_Z\mu_am_Z^2}{s-m_Z^2}\left[\frac{g_Z(v_q^2+a_q^2)M_{ZZ}}{s-m_Z^2} + \frac{eQ_qM_{\gamma Z}v_q}{s}\right]\left[2s(s+m_Z^2-m_S^2)\right].
\end{aligned} \tag{18}$$

Associated ϕW production

At hadron colliders, we can also consider the associated production of a sgoldstino and a W boson, whose partonic cross-section can easily be obtained from the previous ones. For $\phi = P$:

$$\frac{d\sigma}{d\cos\theta}(q\overline{q}' \to PW) = \frac{|\Sigma_{PW}|^2}{32\pi N_c s^2 F^2}\sqrt{(s-m_P^2-m_W^2)^2-4m_P^2m_W^2}\,, \tag{19}$$

where

$$|\Sigma_{PW}|^2 = \frac{g^2|V_{qq'}|^2 M_2^2 s}{8(s-m_W^2)^2}\left(t^2+u^2-2m_P^2m_W^2\right)\,. \tag{20}$$

As in the case of ϕZ production, the cross-section for $\phi = S$ has some additional complications, because of the additional dependence of the SW^+W^- coupling on the higgsino mass parameter μ_a:

$$\frac{d\sigma}{d\cos\theta}(q\overline{q}' \to SW) = \frac{|\Sigma_{SW}|^2}{32\pi N_c s^2 F^2}\sqrt{(s-m_S^2-m_W^2)^2-4m_S^2m_W^2}\,, \tag{21}$$

where

$$\begin{aligned}|\Sigma_{SW}|^2 &= \frac{g^2|V_{qq'}|^2}{4(s-m_W^2)^2}\left[\frac{M_2^2 s}{2}\left[t^2+u^2+2m_W^2(2s-m_S^2)\right]\right.\\ &+ \left.\mu_a^2 m_W^4\left(2s-m_S^2+\frac{tu}{m_W^2}\right)+2\mu_a m_W^2 M_2 s(s+m_W^2-m_S^2)\right]\,.\end{aligned} \tag{22}$$

Vector-boson fusion

The cross-sections for sgoldstino production via vector-boson fusion can be easily calculated, starting from the effective sgoldstino couplings to $\gamma\gamma$, γZ, ZZ and WW. However, their complete analytic expressions are quite involved, and, in analogy with the associated production, also the production via vector boson fusion turns out to be significantly suppressed with respect to the production via gluon-gluon fusion. For these reasons, we omit here a detailed discussion of this production mechanism.

Associated $t\overline{t}\phi$ production

Since the $t\overline{t}\phi$ couplings can be obtained from the Higgs couplings of the SM (or of the MSSM) by the simple rescalings of eqs.(2) and (3), the simplest way to obtain the cross-sections for the associated production of a sgoldstino and a top-antitop pair is to take the corresponding Higgs cross-sections in the SM (or in the MSSM) [17] and to rescale them by the appropriate factor.

Other production mechanisms

As discussed in [6], the effective lagrangian contains some interaction terms that can also lead to the pair-production of a CP–even and a CP–odd sgoldstino, with cross-section

$$\frac{d\sigma}{d\cos\theta}(q\overline{q}\to S\,P)=\frac{(\tilde{m}_q^4+\tilde{m}_{q^c}^4)}{512\pi N_c s^2 F^4}\left[(s-m_S^2-m_P^2)^2-4m_S^2m_P^2\right]^{3/2}\sin^2\theta\,, \qquad (23)$$

where θ is the scattering angle in the center-of-mass frame. For plausible values of the parameters, we expect this cross-section to be suppressed by the large numerical factor and the higher power of the supersymmetry-breaking scale at the denominator. Otherwise, the corresponding signal could be seen as an anomaly in the four-jet sample.

To conclude this section, we comment again on the relative importance of the different production mechanisms. We can see from Fig. 4 that, for the parameter choices of Table 1, the dominant sgoldstino production mechanism at the Tevatron is by far gluon-gluon fusion. The processes of eqs. (6) and (7) are suppressed by roughly four orders of magnitude, and the one of eq. (8) by roughly two more orders of magnitude. Therefore, we shall consider only inclusive signals when discussing the phenomenology at the Tevatron.

4. Phenomenological discussion

The inclusive di-jet signal

Since the most important mechanism for sgoldstino production at the Tevatron is gluon-gluon fusion, and the two-gluon decay mode is the dominant one, it is natural to consider a peak in the dijet invariant mass distribution as a possible signal to be looked for. As a first element to measure the Tevatron sensitivity, we draw in Fig. 5 contours of constant $\sigma(p\overline{p}\to\phi+X)\times BR(\phi\to gg)$ in the $(m_\phi,\sqrt{F})$ plane, for $\sqrt{S}=1.8$ TeV and the two parameter choices of Table 1. Since the curves for $\phi=S$ and $\phi=P$ are almost indistinguishable, we consider only the case $\phi=S$. To account approximately for the NLO QCD corrections [16], we have multiplied the LO result by a K–factor $K=2$.

To interpret the curves of Fig. 5, we need some additional information on the SM backgrounds and on the experimental sensitivity. Fortunately, we can rely on two recent analysis by CDF [18] and D0 [19], devoted to the search of new particles decaying to dijets, and thus applicable to sgoldstinos. Using 106 pb^{-1} of data collected at $\sqrt{S}=1.8$ TeV, and requiring that both jets have pseudorapidity $|\eta|<2.0$ and a scattering angle in the dijet center-of-mass frame $|\cos\theta^*|\equiv|\tanh[(\eta_1-\eta_2)/2]|<2/3$, CDF plots and tabulates the 95% c.l. upper limit on the cross-section times branching ratios for narrow resonances ($\Gamma/M<0.1$) decaying into dijets. D0 uses 104 pb^{-1}, requires $|\eta|<1.0$ and $|\eta_1-\eta_2|<1.6$, and plots a 95% c.l. upper limit on the cross-section times branching ratio times acceptance

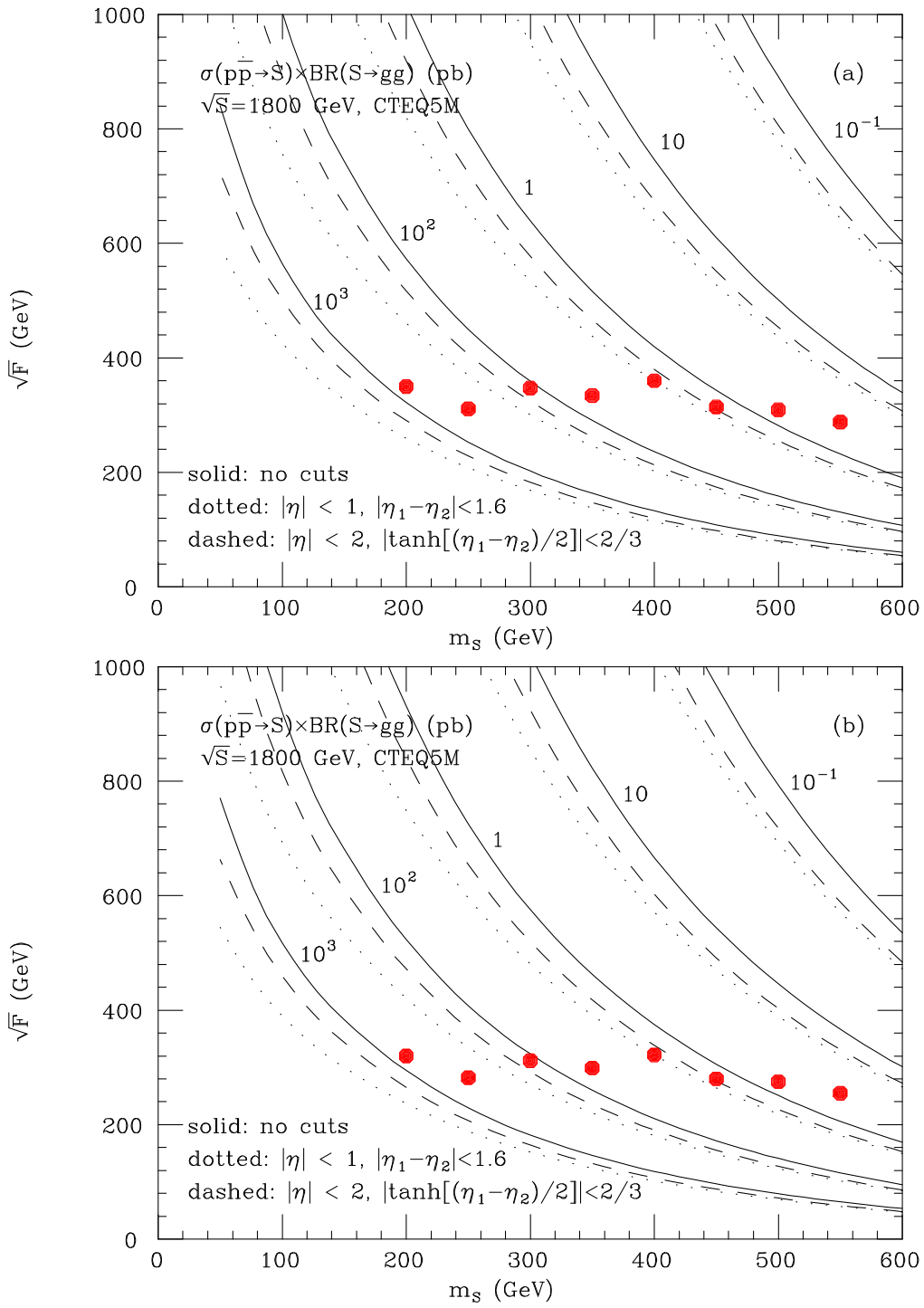

Figure 5: *Lines corresponding to fixed values of* $\sigma(p\overline{p} \to S + X) \times BR(S \to gg) = 10^{-1,0,1,2,3}$ pb, *for* $\sqrt{S} = 1.8$ TeV *and* $K = 2$, *in the* $(m_S, \sqrt{F})$ *plane and for the two parameter choices of Table 1. Solid lines: no cuts. Dashed lines: 'CDF' cuts. Dotted lines: 'D0' cuts. Fat dots: tentative estimate of the Tevatron sensitivity after run I.*

for three representative models of new physics. We have used the published CDF and D0 data and our calculation of the sgoldstino cross-sections and branching ratios to draw in Fig. 5 a sequence of fat dots, representing our tentative estimate of the Tevatron sensitivity after run I. This line was obtained by selecting, for each value of the sgoldstino mass (from 200 to 600 GeV, in steps of 50 GeV), the more stringent of the CDF and D0 limits on $\sqrt{F}$, obtained under the assumption $\Gamma_\phi/m_\phi < 0.1$. By comparing with Fig. 3, however, we can see that for increasing sgoldstino masses this assumption is more and more strongly violated. As a result, we expect to have made a stronger and stronger overestimate of the present bounds for increasing mass values in the region above 300 GeV.

To have an idea of the Tevatron sensitivity after run II, for each given value of the sgoldstino mass we can rescale the corresponding value of $\sqrt{F}$ by a factor $20^{1/8} \simeq 1.5$. This amounts to making the naïve assumptions that the cross-section does not vary much when changing $\sqrt{S}$ from 1.8 to 2.0 TeV, and that the error in the cross–section measurement will scale as $1/\sqrt{L}$, where L is the integrated luminosity.

The inclusive di-photon signal

In the case of the SM and MSSM neutral Higgs bosons, the two-photon decay mode has a very suppressed branching ratio, at most $\mathcal{O}(10^{-3})$ in the mass region between 100 and 150 GeV, and much smaller for larger masses. As a result, the diphoton signal is marginal for Higgs searches at the Tevatron, and it is much more convenient to exploit other decay modes, in conjunction with associated production mechanisms. In contrast, sgoldstinos have diphoton branching ratios well above $\mathcal{O}(10^{-2})$ over the whole mass range between a few and 1000 GeV, and possibly larger inclusive production cross-sections, so we can expect the inclusive diphoton signal to play a major rôle in sgoldstino searches at the Tevatron.

As a first piece of information, we display in Fig. 6 contours of constant $\sigma(p\overline{p} \to \phi + X) \times BR(\phi \to \gamma\gamma)$ in the $(m_\phi, \sqrt{F})$ plane, for $\sqrt{S} = 1.8$ TeV and the two parameter choices of Table 1. Since the curves for $\phi = S$ and $\phi = P$ are almost indistinguishable, we consider only the case $\phi = S$. In this case, the NLO QCD corrections [16] are not included, since they have two competing effects that approximately cancel: an increase in the inclusive production cross-section, but also a similar increase in the two-gluon partial width, which correspondingly reduces the two-photon branching ratio.

To interpret the curves of Fig. 6, we need some additional information on the SM backgrounds and on the experimental sensitivity. Again, we can rely on some recent analysis by CDF [20] and D0 [21], as well as on some useful information contained in a recent study for run II [22]. The CDF study uses 100 pb^{-1} of data collected at $\sqrt{S} =$ 1.8 TeV, and requires that both photons have pseudorapidity $|\eta| < 1$ and transverse energy $E_T > 22$ GeV. Since the study looks specifically at the invariant mass distribution of diphotons above 50 GeV, it is relatively simple to translate its results into a tentative sensitivity curve in the $(m_\phi, \sqrt{F})$ plane. The D0 studies were performed with slightly different goals, and some work would be required in order to optimize their data analysis

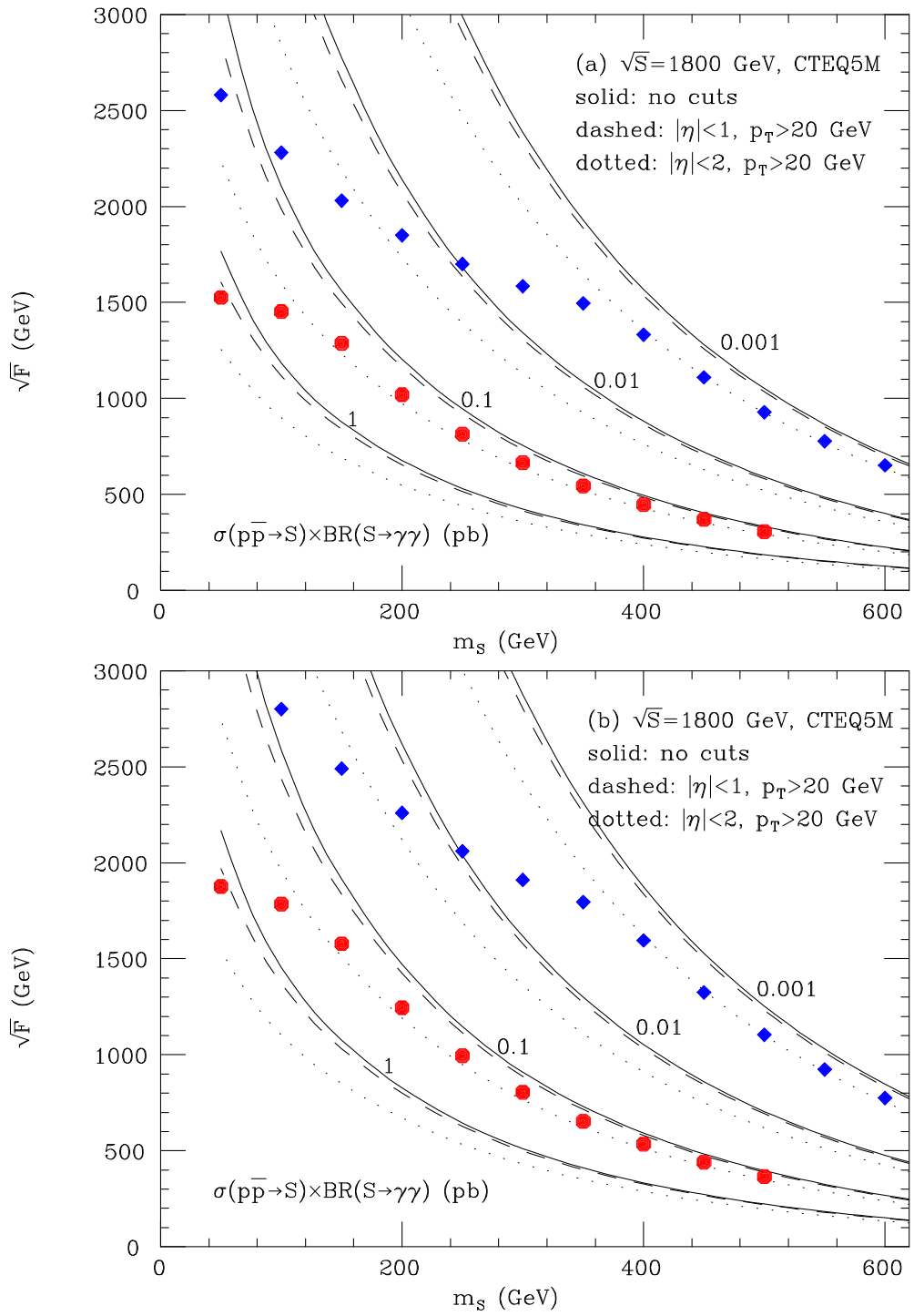

Figure 6: *Lines corresponding to fixed values of* $\sigma(p\overline{p} \to S + X) \times BR(S \to \gamma\gamma) = 10^{-3,-2,-1,0}$ pb, *for* $\sqrt{S} = 1.8$ TeV *and* $K = 1$, *in the* $(m_S, \sqrt{F})$ *plane and for the two parameter choices of Table 1. The fat dots and diamonds represent our tentative estimates of the Tevatron sensitivity after run I and after run II, respectively.*

for setting limits on sgoldstinos. On the contrary, the study in [22], performed with the cuts $|\eta| < 2$ and $E_T > 20$ GeV, comes with an analytical formula for the background and can be easily used to obtain a first, rough estimate of the run II sensitivity. For example, following [22], we can assume a diphoton identification efficiency $\epsilon = 0.8$ and combine the finite sgoldstino width and the experimental resolution in the diphoton invariant mass by defining a quantity $[\Delta/(1\ \mathrm{GeV})] = \sqrt{[\Gamma_\phi/(1\ \mathrm{GeV})]^2 + (0.35)^2\,[m_\phi/(1\ \mathrm{GeV})]}$. We can then ask that, if S is the number of signal events and B the number of background events in a window of width $1.2\,\Delta$ centered around m_ϕ, either $S/\sqrt{B} > 5$ (if $B > 1$) or $S > 5$ (if $B < 1$). Doing so, and leaving a more detailed and reliable analysis to our experimental colleagues, we could draw in Fig. 6 two series of fat dots and diamonds, representing our tentative estimates of the Tevatron sensitivities after run I and after run II, respectively. A more sophisticated study could proceed along the lines of [23] and make full use of the double differential cross-section in the diphoton invariant mass and in the scattering angle, to take into better account the finite-width effects (important for large sgoldstino masses) and to reduce the dependence on the cuts (important for small sgoldstino masses). For our present purposes, however, it is sufficient to observe that, for the two parameter choices of Table 1, searching for the diphoton signal is by far the most powerful way of constraining the sgoldstino parameter space. [3]

Whilst the searches for very massive sgoldstinos should be relatively straightforward, an interesting phenomenological question is how to extend and maximize the Tevatron reach in the region of small masses, $m_\phi \ll 100$ GeV. In this respect, it may be useful to relax as much as possible the trigger and selection requirements on the photon transverse energy. Also, in the region of very small masses, the associated production mechanisms with electroweak gauge bosons may play a useful role.

Acknowledgements. We would like to thank A. Brignole, A. Castro, G. Landsberg, M.L. Mangano, M. Spira and D. Wood for useful discussions and suggestions.

References

[3] The range of accessible sgoldstino masses may extend beyond the right border of Fig. 6. To reliably explore that region, however, we should take into account the effects of sgoldstino decays into neutralinos, charginos and eventually gluinos.

[1] G.R. Farrar and P. Fayet, Phys. Lett. B76 (1978) 575;
P. Fayet, Phys. Lett. B84 (1979) 421, B86 (1979) 272, B117 (1982) 460 and B175 (1986) 471.

[2] O. Nachtmann, A. Reiter and M. Wirbel, Z. Phys. C27 (1985) 577;
T. Bhattacharya and P. Roy, Phys. Rev. Lett. 59 (1987) 1517 + (E) 60 (1988) 1455;
D.A. Dicus, S. Nandi and J. Woodside, Phys. Rev. D43 (1991) 2951 and Phys. Lett. B258 (1991) 231;
J.L. Lopez, D.V. Nanopoulos and A. Zichichi, Phys. Rev. Lett. 77 (1996) 5168 and Phys. Rev. D55 (1997) 5813;
J. Kim et al., Phys. Rev. D57 (1998) 373.

[3] A. Brignole, F. Feruglio and F. Zwirner, Nucl. Phys. B501 (1997) 332; Phys. Lett. B438 (1998) 89; Nucl. Phys. B516 (1998) 13 + (E) B555 (1999) 653;
A. Brignole, F. Feruglio, M.L. Mangano and F. Zwirner, Nucl. Phys. B526 (1998) 136 and erratum [hep-ph/9801329].

[4] A. Brignole, E. Perazzi and F. Zwirner, JHEP 9909 (1999) 002.

[5] T. Bhattacharya and P. Roy, Phys. Rev. D38 (1988) 2284;
D.A. Dicus, S. Nandi and J. Woodside, Phys. Rev. D41 (1990) 2347;
D.A. Dicus and P. Roy, Phys. Rev. D42 (1990) 938;
D.A. Dicus and S. Nandi, Phys. Rev. D56 (1997) 4166.

[6] E. Perazzi, G. Ridolfi and F. Zwirner, hep-ph/0001025, to appear in Nuclear Physics B (2000).

[7] E. Anashkin, P. Checchia, F. Mazzucato and E. Piotto (DELPHI Collaboration), note DELPHI 2000-013 CONF 334.

[8] G. Abbiendi et al. (OPAL Collaboration), Phys. Lett. B465 (1999) 303.

[9] Y. Okada, M. Yamaguchi and T. Yanagida, Prog. Theor. Phys. Lett. 85 (1991) 1;
J. Ellis, G. Ridolfi and F. Zwirner, Phys. Lett. B257 (1991) 83 and B262 (1991) 477;
H.E. Haber and R. Hempfling, Phys. Rev. Lett. 66 (1991) 1815.

[10] A. Brignole et al., work in progress.

[11] J. A. Bagger, A. F. Falk and M. Swartz, Phys. Rev. Lett. 84 (2000) 1385;
B. A. Kniehl and A. Sirlin, hep-ph/9907293v3.

[12] N. Arkani-Hamed, S. Dimopoulos and G. Dvali, Phys. Lett. B429 (1998) 263 and Phys. Rev. D59 (1999) 086004;
I. Antoniadis, N. Arkani-Hamed, S. Dimopoulos and G. Dvali, Phys. Lett. B436 (1998) 257.

[13] L. Randall and R. Sundrum, Phys. Rev. Lett. 83 (1999) 3370 and 83 (1999) 4690.

[14] G.F. Giudice, R. Rattazzi and J.D. Wells, hep-ph/0002178;
U. Mahanta and A. Datta, hep-ph/0002183;
S. Bae, P. Ko, H.S. Lee and J. Lee, hep-ph/0002224.

[15] H. L. Lai *et al.* (CTEQ Collaboration), Eur. Phys. J. C12 (2000) 375.

[16] M. Spira, A. Djouadi, D. Graudenz and P.M. Zerwas, Nucl. Phys. B453 (1995) 17, and references therein.

[17] M. Spira, Fortsch. Phys. 46 (1998) 203 and hep-ph/9810289.

[18] F. Abe et al. (CDF Collaboration), Phys. Rev. D55 (1997) 5263.

[19] B. Abbott et al. (D0 Collaboration), FERMILAB-CONF-97-356-E.

[20] P.J. Wilson (for the CDF Collaboration), FERMILAB-CONF-98-213-E.

[21] B. Abbott et al. (D0 Collaboration), Phys. Rev. Lett. 81 (1998) 524;
Wei Chen, Ph.D. Thesis, available at http://www-d0.fnal.gov/results.

[22] G. Landsberg and K.T.Matchev, hep-ex/0001007v2.

[23] K. Cheung and G. Landsberg, hep-ph/9909218.